

N94-22741

## Aeronautical Audio Broadcasting via Satellite

Forrest F. Tzeng  
COMSAT Laboratories  
22300 Comsat Drive  
Clarksburg, MD 20871-9475, U.S.A.  
Tel: (301)428-4659 Fax: (301)428-4534

### ABSTRACT

A system design for aeronautical audio broadcasting, with C-band uplink and L-band downlink, via Inmarsat space segments is presented. Near-transparent-quality compression of 5-kHz bandwidth audio at 20.5 kbit/s is achieved based on a hybrid technique employing linear predictive modeling and transform-domain residual quantization. Concatenated Reed-Solomon/convolutional codes with quadrature phase shift keying are selected for bandwidth and power efficiency. RF bandwidth at 25 kHz per channel, and a decoded bit error rate at  $10^{-6}$  with  $E_b/N_o$  at 3.75 dB, are obtained. An interleaver, scrambler, modem synchronization, and frame format were designed, and frequency-division multiple access was selected over code-division multiple access. A link budget computation based on a worst-case scenario indicates sufficient system power margins. Transponder occupancy analysis for 72 audio channels demonstrates ample remaining capacity to accommodate emerging aeronautical services.

### INTRODUCTION

The field of mobile satellite communications has experienced rapid growth in recent years. Compared to the maritime and land mobile segments, the aeronautical segment of mobile satellite systems is relatively new. However, many new aeronautical services have emerged, and this trend is expected to continue. Some examples include air phone, in-flight news, in-flight customs clearance, and aeronautical facsimile (aero fax).

In this study, schemes were designed for low-rate audio coding, coded modulation, and digital transmission architecture to support live audio program broadcasting to commercial aircraft via the Inmarsat space segments. Due to the bandwidth and power limitations of the Inmarsat segments, the audio programs targeted for the current application include talk shows, sports coverage, news, commentaries, and weather, as well as intermission music. Consequently, a monaural audio signal of 5-kHz bandwidth (AM-quality audio) was selected. The information source also includes a subband broadcast data channel with a data rate range from 300 to 2,400 bit/s.

Several system design constraints were considered. These included use of the existing Inmarsat-Aero aircraft earth station (AES) antenna subsystem to minimize customer cost, simple and low-cost airborne subsystem (re-

ceiver) hardware, and applicability to both the Inmarsat-2 and Inmarsat-3 space segments. In addition, the RF bandwidth per audio channel had to be a multiple of 2.5 kHz to be consistent with the Inmarsat systems.

This paper describes a low-rate audio coding scheme that achieves near-transparent-quality compression of 5-kHz bandwidth audio at 20.5 kbit/s. Error protection strategies for compressed audio and data are also presented. Candidate coded modulation schemes are compared in terms of their power and bandwidth efficiency, and designs for an interleaver, scrambler, modem synchronization, and frame format are discussed. Multiple-access techniques are then compared, and link budget computation and transponder occupancy analysis results are presented.

### AUDIO COMPRESSION AND ERROR PROTECTION

#### Audio Compression

The technique for adaptive predictive coding with transform-domain quantization (APC-TQ) [1] presented here combines time-domain linear prediction modeling and transform-domain quantization of the prediction residual signal. The APC-TQ technique is efficient in exploiting the nonuniform power spectral distribution that exists in audio signals. It also permits the direct implementation of auditory noise-masking techniques based on auditory characteristics, to maximize the perceived quality of the reconstructed audio.

The audio signal is band-limited to 5 kHz and sampled at a rate of 10.24 kHz. A frame size of 256 samples is used. The power spectrum model for each frame of audio samples is a product of two terms: a short-term model which represents coarse or envelope spectral variations, and a long-term model which represents fine or harmonic spectral variations. The resulting power spectrum model is used to determine the bit allocation for residual quantization.

Short-term prediction is accomplished by predicting each sample based on a weighted sum of a few samples immediately preceding it. A fifth-order linear predictive model is computed using the autocorrelation method [2]. The five filter coefficients are converted into line spectrum frequencies (LSFs) [3] and scalarly quantized using 24 bits overall (with 5, 5, 5, 5, and 4 bits for the five LSFs, respectively). The LSFs were found to have good

properties for quantization. In addition, they allow easy channel error concealment in terms of guaranteed filter stability and minimum filter distortion when in error.

Long-term prediction consists of estimating the optimum long-term prediction delay (*i.e.*, pitch) and predicting each sample from a weighted sum of the three samples located around the delay. The delay is estimated by computing the autocorrelation function of the short-term prediction error signal over the delay range from 20 to 256 samples. The optimum delay is indicated by the location of the peak of the autocorrelation function, and the delay value is coded using 8 bits. The long-term prediction parameters are selected from a code book of 128 parameter sets [4], based on the criterion of minimizing the long-term prediction error power over the analysis frame.

The residual signal after short- and long-term prediction is quantized next. The 256 samples of the residual signal are transformed using a discrete cosine transform (DCT), and are quantized using a total of 465 bits. These bits are nonuniformly allocated based on the power spectral estimate obtained using the short- and long-term prediction parameters. Scalar Max quantizers [5] optimized for zero-mean, univariate Gaussian distribution are employed. A scaling parameter is determined in order to scale the DCT coefficients to unit variance. The parameter is then quantized logarithmically using 8 bits.

At the decoder, the short-term and long-term prediction parameters are decoded and used to determine the bit allocation. Based on this allocation, the transform coefficients are decoded and inverse DCT is applied to obtain the quantized version of the residual signal. This signal excites the cascade of long- and short-term synthesis filters to reconstruct the audio signal. At 20.5 kbit/s, a near-transparent-quality coded 5-kHz audio signal was reconstructed.

### Error Protection

For aeronautical broadcast applications, the uplink C-band channel (ground earth station [GES] to satellite) and the downlink L-band channel (satellite to aeronautical earth station [AES]) can be modeled as an additive white Gaussian noise (AWGN) channel and a Rician channel (with a Rice factor of  $K = 10$ ) [6], respectively. For broadcast audio, the transmission time delay is not as critical as for conversational speech. Therefore, an interleaver with an appropriate interleaving length can be used so that the multipath Rician fading downlink channel effectively becomes AWGN.

The use of convolutional codes is a proven technique for error correction under AWGN channel conditions. In this study, an inner-layer convolutional code was selected for both the audio signal and broadcast data. A target decoded bit error rate (BER) of  $10^{-3}$  was selected for this inner-layer error protection scheme. The decoded BER is used as a basis for comparing the power and bandwidth

efficiency of several candidate coding and modulation schemes, as described below. Both the audio and data information were further protected by using an additional outer-layer error protection scheme to lower the overall decoded BER to less than  $10^{-6}$ . At this BER, the subjective degradation to the audio is imperceptible.

Two approaches were considered for the design of the outer-layer error protection. The first approach treats audio and data separately and uses a Reed-Solomon (RS) code as the outer code to form a concatenated code with the inner convolutional code to protect data. Audio is protected using an unequal-error-protection (UEP) method. In UEP, the more sensitive bits of audio are given a higher level of error protection, while less-sensitive bits are given a lower level or even no error protection. The second approach treats audio and data as a single entity, and both are protected using an outer RS code, as in the first approach for data.

To attempt the first approach, a UEP scheme was devised which included (23, 12) Golay codes, (7, 4) Hamming codes, and parity checks as component codes, augmented by several judiciously designed error detection and error concealment techniques. This scheme provided sufficient protection for most bits of the short-term filter coefficients, pitch, long-term filter coefficients, and scaling parameter. However, there were no bits available to protect the remaining bits.

Work with the second approach for outer-layer error protection revealed that it was more efficient. Given the available redundancy, the concatenated code achieves the desired decoded BER of  $10^{-6}$  for both audio and data at a very reasonable energy-per-bit to noise-power density ratio,  $E_b/N_0$ . This approach also allows a simpler decoder design, since only one RS decoder and one outer interleaver are necessary. An RS(255, 229) code over a Galois field GF(256) was finally selected. This code can correct 13 symbol (byte) errors. Figure 1 is a block diagram of the overall transmission system.

## CODING AND MODULATION

### Coded Modulation

In selecting an appropriate inner-layer coded modulation scheme, only quadrature phase shift keying (QPSK), its variants, and octal phase shift keying (OPSK) were considered. These are well-known, proven techniques for satellite communications. Quadrature amplitude modulation schemes are not suitable for non-linear channel operations, while continuous-phase frequency shift keying and its variants, such as multi- $h$  codes, are complicated, and their performance does not justify use in this application.

Several candidate coded modulation schemes were examined (Table 1). For separate coding and modulation schemes, rate 1/2, 2/3, 3/4, and 5/6 coded QPSK were considered. For combined coding and modulation

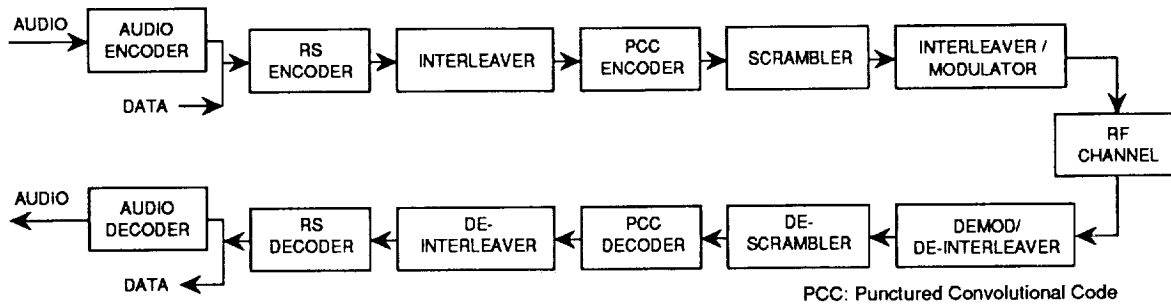


Figure 1. Digital Transmission System Block Diagram

Table 1. Candidate Coded Modulation Schemes

CODED MODULATION	$E_b/N_0$ (dB) @ $10^{-3}$	RF BANDWIDTH (kHz)
1/2 QPSK	3	37.5
2/3 QPSK	3.5	30
3/4 QPSK	4	25
5/6 QPSK	4.6	25
2/3 OPSK (TCM)	5	20
5/6 OPSK (TCM)	5.7	17.5
2/3 D-OPSK (TCM)	8.4	20

schemes, rate 2/3 coded OPSK, differential OPSK (D-OPSK), and rate 5/6 coded OPSK were considered.

For the power estimates, an inner-layer decoded BER of  $10^{-3}$  was assumed. For separate coding and modulation schemes, all convolutional codes were assumed to have a constraint length of 6 with 3-bit soft decision. In trellis-coded modulation (TCM) schemes, 16-state codes were assumed. The higher-rate convolutional codes (rate 2/3, 3/4, and 5/6) used in separate coding and modulation schemes were realized by using punctured convolutional codes [7] based on the rate 1/2 optimum code [8], to reduce decoding complexity.

The RF bandwidth estimates assumed a 35-percent rolloff factor for a square-root, raised-cosine shaping filter, and a 1.375-kHz guard band (0.6875 kHz at each side) for each carrier. The guard band value was selected based on the maximum AES receiver frequency error specified in the Inmarsat-Aero "System Definition Manual" (SDM) [9]. Also, a data rate of 1 kbit/s was added for modem synchronization and framing redundancies. These bits are used as preambles, unique words (UWs), audio channel ID information (for broadcast channel scanning), and flush bits. The computed bandwidth requirements were converted into multiples of 2.5 kHz to meet system requirements.

Based on the power and bandwidth requirements shown, two candidate coded modulation schemes were considered: rate 2/3 coded OPSK (TCM) and rate 3/4 coded QPSK. Rate 2/3 coded OPSK is more bandwidth-efficient, while rate 3/4 coded QPSK is more power-efficient. Rate 3/4 coded QPSK was selected, since it requires 1 dB less power, and the aeronautical

downlink is power-limited. Also, with increased bandwidth, carrier power can be increased without changing the power density. This is an important factor in frequency planning.

### Interleaving and Synchronization

Two block interleavers were employed. The inner interleaver decorrelates burst errors created by the RF fading channel, while the outer interleaver decorrelates burst errors at the Viterbi decoder output. For the RF fading channel, the maximum fade duration had been shown to be about 20 ms [6], which corresponds to about 680 bits. For the rate 3/4 Viterbi decoder, the maximum burst length is less than 35 bits [10].

For inner interleaving, the number of rows (NR) was selected to be 775 bits, in order to exceed the maximum fade duration. The number of columns (NC) can theoretically be selected to be equal to the Viterbi decoding length, which is about six times the constraint length. However, in practice a larger NC must be used, especially for higher-rate codes such as the rate 3/4 code selected for this application [10]. An NC of 88 bits was used. The selection of these two particular values for NR and NC was based on the frame format described in the next subsection.

For the outer interleaver, NR was selected to be 25 bits and NC was selected as the RS code length, which is 255 bytes (2,040 bits). The 25-bit NR was selected for two reasons. First, it was desired not to introduce too much interleaving delay. Second, for consistency with the Inmarsat-Aero SDM, a frame size of 500 ms was selected. Given this frame size, it was decided that 51 kbit/s was a good value for both the outer interleaver size ( $2,040 \times 25$ ) and the incoming data rate ( $25.5 \text{ kbit/s} \times 2 \text{ s}$ ).

In terms of synchronization, the modem needs to be robust at a low carrier-to-noise power density ratio,  $C/N_o$ , in the presence of L-band Doppler shifts varying between  $\pm 2$  kHz. In addition, multipath fading is prevalent at elevation angles below  $10^\circ$ , and signal can be blocked by the aircraft tail structure. Because coherent detection is used for power efficiency, reliable carrier frequency/phase acquisition and tracking with a minimum of cycle slips is required. A channel scanning capability is also

desired so that a receiver can scan each of the available aeronautical channels.

The channel rate after rate 3/4 convolutional encoding, excluding framing bits, is 34 kbit/s. To simplify equipment design and implementation, the channel rate is required to be a submultiple of a 5.04-MHz master clock, for compatibility with other Inmarsat-Aero channel unit bit rates. A channel rate of 35 kbit/s meets this requirement and allows 3-percent capacity for framing overhead bits.

The bit rate of the system is approximately 67 percent faster than the 21-kbit/s Inmarsat-Aero standard channel. However, this is an advantage in terms of carrier synchronization and tracking, because frequency variations are a smaller percentage of the bit rate. The maximum AES received frequency error is specified as  $\pm 346$  Hz, plus the AES Doppler shift of  $\pm 2$  kHz, for a total uncertainty of  $\pm 2,346$  Hz. Since this is less than 7 percent of the channel rate, conventional carrier tracking methods such as a Costas loop or decision-directed carrier tracking loop can be used. Symbol timing tracking is also straightforward, and a conventional symbol transition detector can be employed. As specified in the SDM, a scrambler is used for energy dispersal and to assist in symbol synchronization.

### Frame Format

The channel frame format is shown in Figure 2. To maintain system compatibility with the Inmarsat-Aero SDM, the frame duration is chosen to be 500 ms. Each frame contains its own preamble and an 88-bit UW, which is identical to that used on the current Inmarsat-C channel. The preamble consists of 160 bits of unmodulated carrier for carrier synchronization, followed by a 160-bit alternating 0101 pattern for clock synchronization. The occurrence of these bits in every frame permits rapid acquisition and reacquisition after a fade or tail blockage. Each frame also contains a 16-bit station ID

field, which allows a receiver to perform station verification in order to facilitate rapid channel scanning.

The inner and outer forward error correction (FEC) interleavers were both chosen to have a time span of 2 s. Thus, a 2-s superframe structure was defined consisting of four 500-ms frames. A different 88-bit UW, denoted UW', is employed to mark the first frame of a superframe. A 12-bit frame counter field, denoted FC, immediately follows the UW and consists of a 4-bit frame counter repeated three times for bit error immunity.

Figure 3 is a block diagram of the procedure used to pack the program audio and secondary data channel bits into 500-ms frames. The program audio channel has an information rate of 20.5 kbit/s, and the data channel is assumed to have an information rate of 2,400 bit/s. If lower data channel rates are desired, the data field will have to be packed with enough dummy bits to achieve a 2,400-bit/s rate. To assemble a frame, 2 s of program audio (41,000 bits) and 2 s of secondary data (4,800 bits) are buffered in memory. It is assumed that the actual frame assembly is much faster than real time, so that the total transmitter delay is not much greater than 2 s. While the data are being processed, the next superframe is being buffered in memory for subsequent frame assembly.

### TRANSMISSION SYSTEM ARCHITECTURE

#### Multiple Access

Due to the circuit-switched nature of broadcast audio programs, time-division multiple access (TDMA) was not considered. However, frequency-division multiple access (FDMA) and code-division multiple access (CDMA) methods were carefully compared.

CDMA possesses several advantages, including the possibility of overlay on top of narrowband users; system flexibility through the use of programmable codes; multipath rejection and interference suppression capabilities; and graceful degradation with an increased number of

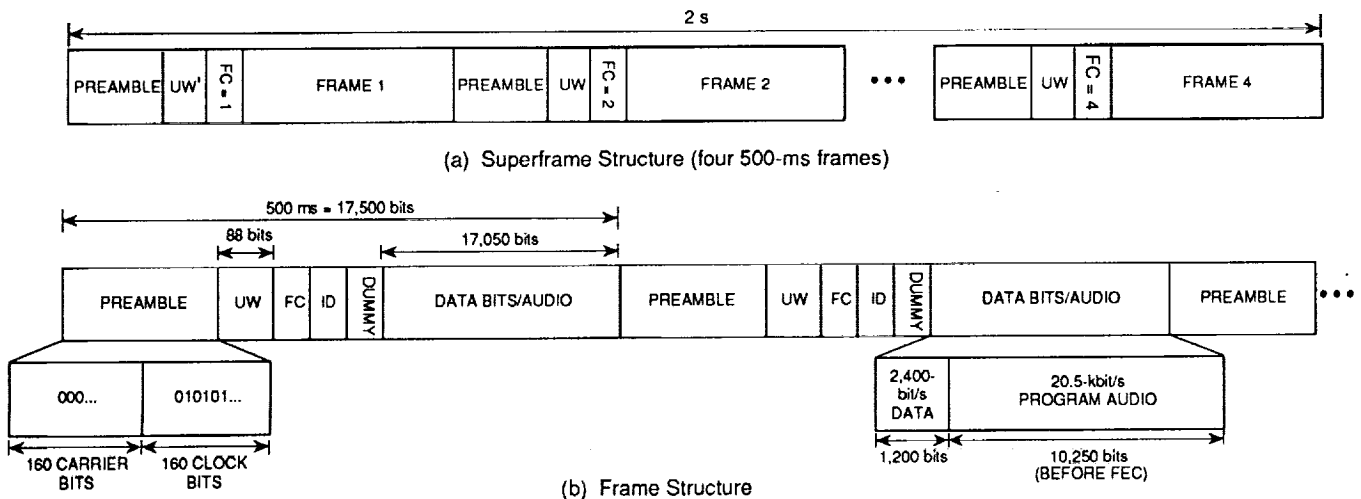


Figure 2. Frame Format

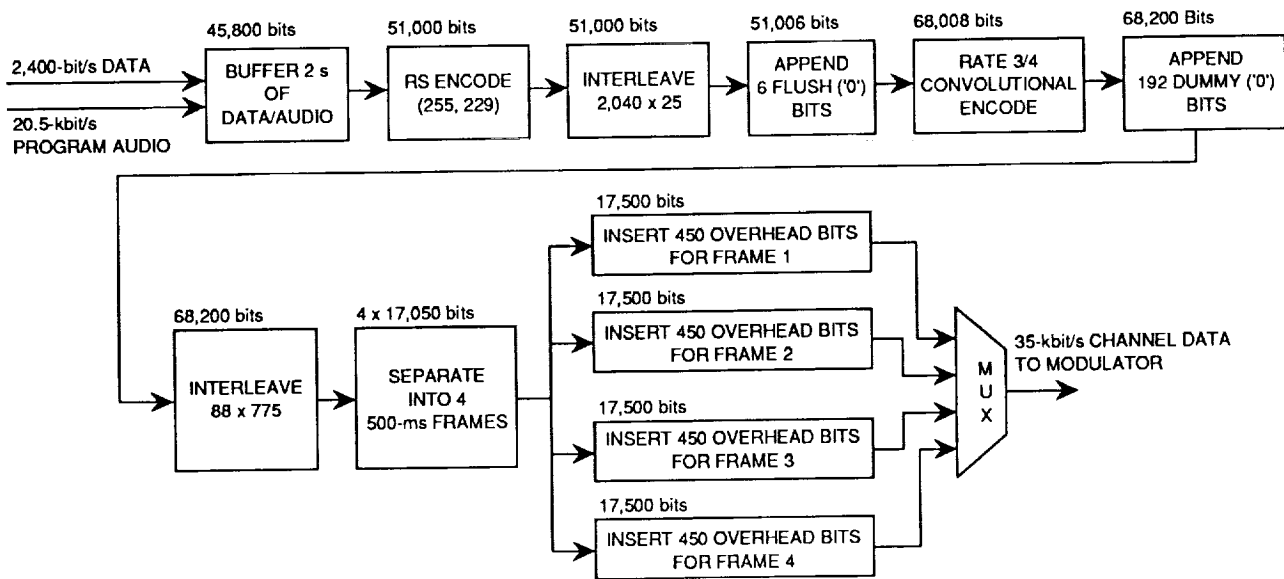


Figure 3. Frame Assembly

active broadcast co-channels. However, the small channelized transponder bandwidth available (1.4 MHz maximum for Inmarsat-2, as described later), coupled with the high channel data rate, makes the processing gain very small for a direct-sequence CDMA system. Although a frequency-hopping CDMA system does not require contiguous bandwidth, the necessary frequency synthesizers would increase aircraft receiver complexity and cost. This consideration also applies to direct-sequence CDMA systems, which require additional circuits for code acquisition and tracking.

In view of the above considerations, FDMA/SCPC (single channel per carrier) was selected. Its implementation is relatively simple and is compatible with most of the existing Inmarsat traffic. Since the aero broadcasting system is downlink-limited, the intermodulation interference in an FDMA system does not critically limit system performance. However, it is still advisable to reduce intermodulation interference. This can be achieved by using an optimized frequency plan, examples of which are given in References 11 and 12.

### Link Budget

A link budget (Table 2) was prepared for Inmarsat-2 satellite links. An elevation angle of 5° (a worst-case scenario) was assumed for AES, with a system margin of 3 dB. The concatenated RS/punctured convolutional code was simulated in software, and it was determined that an  $E_b/N_o$  of about 3.75 dB is required in order to achieve the desired decoded BER of  $10^{-6}$ .

The link analysis further assumes that there is no adjacent satellite interference or co-channel interference involved. The adjacent channel interference effect is also assumed to be offset by the pulse-shaping filter and the guard bands. Note that this analysis is based on

Table 2. Link Budget Analysis

PARAMETER	VALUE
<b>Uplink (GES to Satellite)</b>	
Frequency	6.44 GHz
GES Elevation	5°
GES Tx EIRP	65 dBW
Path Loss (incl. atmos. loss)	201.3 dB
Satellite Rx $G/T$	-14 dB/K
Uplink $C/N_o$	75.3 dB-Hz
<b>Satellite</b>	
Satellite Gain	161.3 dB
Satellite $C/IM_o$	67.0 dB-Hz
<b>Downlink (Satellite to AES)</b>	
Frequency	1.545 GHz
AES Elevation	5°
Satellite Tx EIRP	25 dBW
Path Loss (incl. atmos. loss)	188.9 dB
AES Rx $G/T$	-13 dB/K
Downlink $C/N_o$	51.7 dB-Hz
<b>Link Performance</b>	
Overall $C/N_o$	51.6 dB-Hz
Required $E_b/N_o$ at $10^{-6}$	3.75 dB
Data Rate (22.9 kbit/s)	43.6 dB
Miscellaneous Loss (modem loss and random losses)	1.25 dB
Link $C/N_o$ Requirement	48.6 dB-Hz
System Margin	3.0 dB

Inmarsat-2 satellite specifications. For Inmarsat-3 satellites, the link budget could show significantly better power capacity. In addition, if the flight route is such that the elevation angle is significantly greater than 5°, the 3-dB link margin could be achieved with a lower GES transmit effective isotropically radiated power (EIRP).

## Aero-Band Occupancy

For initial system operation, it is assumed that three channels will be provided for each Inmarsat signatory in the Atlantic Ocean Region (AOR) East, AOR West, Pacific Ocean Region (POR), and Indian Ocean Region (IOR). There are six signatories in each region, for a total of 72 planned channels.

For the Inmarsat-3 space segment, the uplink C-band has a 29-MHz bandwidth (6,425 to 6,454 MHz), from which the aeronautical portion is allocated a 10-MHz bandwidth (6,440 to 6,450 MHz). The downlink L-band has a 34-MHz bandwidth (1,525 to 1,559 MHz), from which the aeronautical portion is also allocated a 10-MHz bandwidth (1,545 to 1,555 MHz). However, each of the two 10-MHz bands is divided into three bands of 3, 3, and 4 MHz, respectively, separated by some guard bands (1.2 and 1.4 MHz, 1.2 and 1.4 MHz, 2.3 and 1.3 MHz, respectively). Thus, the actual usable bandwidth is only 8.8 MHz.

For the Inmarsat-2 space segment, the uplink aeronautical C-band is allocated a 3-MHz bandwidth (6,440 to 6,443 MHz), and the downlink aeronautical L-band is also allocated a 3-MHz bandwidth (1,545 to 1,548 MHz). Each of these two bands is divided into two bands of 1.2 and 1.4 MHz, separated by a guard band. Consequently, the actual usable bandwidth is 2.6 MHz.

The aero-band occupancy percentage,  $m$ , was defined as the ratio of the total bandwidth required to support the 72 audio broadcast channels vs the total usable bandwidth allocated for aeronautical services. For the selected coded modulation scheme, the required RF bandwidth is 25 kHz for each audio channel. The corresponding occupancy percentage is then  $m = 69.2$  percent for Inmarsat-2, and  $m = 20.5$  percent for Inmarsat-3. These percentages are reasonable for high-data-rate audio programs, especially for Inmarsat-3 satellites. Thus, there should be ample system capacity remaining to accommodate many emerging aeronautical services.

## CONCLUSIONS

A system design to support aeronautical broadcast of audio programs via the Inmarsat-2 and -3 space segments has been presented. Near-transparent-quality compression of 5-kHz bandwidth audio at 20.5 kbit/s were described. Candidate error protection strategies and coded modulation schemes were carefully compared to achieve robust performance with bandwidth and power efficiency. Designs for an interleaver, scrambler, modem synchronization, and frame format were presented, and the considerations used in selecting FDMA for multiple access were discussed. Results of the link budget computation and transponder occupancy analysis were also presented.

The designed system currently supports the transmission of AM broadcast-quality audio programs to commer-

cial aircraft equipped with high-gain AES antenna subsystems. With rapid advances in audio compression technology, higher quality broadcast audio programs such as near-FM audio could be supported in the near future, using the same transmission system described here. The system might also be capable of supporting the transmission of AM-quality audio programs to aircraft equipped with low-gain omnidirectional AES antenna subsystems. By using Inmarsat-3 spot beams, near-FM-quality audio broadcasts to aircraft with low-gain AES antennas might also be achievable.

## ACKNOWLEDGMENTS

This paper is based on work performed at COMSAT Laboratories under the sponsorship of the Communications Satellite Corporation. The author wishes to acknowledge his colleague H. Chalmers for his work on synchronization and frame format design.

## REFERENCES

- [1] B. R. U. Bhaskar, "Adaptive Prediction With Transform Domain Quantization for Low Rate Audio Coding," IEEE ASSP Workshop on Applications of Signal Processing to Audio and Acoustics, New Paltz, NY, *Proc.* (unpaginated), October 1991.
- [2] L. R. Rabiner and R. W. Schafer, *Digital Processing of Speech Signals*, Englewood Cliffs, NJ: Prentice-Hall, 1978.
- [3] G. Kang and L. Fransen, "Application of Line-Spectrum Pairs to Low-Bit-Rate Speech Encoders," IEEE International Conference on Acoustics, Speech, and Signal Processing, Tampa, FL, *Proc.*, pp. 244-247, March 1985.
- [4] Y. Linde, A. Buzo, and R. Gray, "An Algorithm for Vector Quantizer Design," *IEEE Transactions on Communications*, Vol. COM-28, No. 1, pp. 84-95, January 1980.
- [5] J. Max, "Quantizing for Minimum Distortion," *IRE Transactions on Information Theory*, Vol. IT-6, pp. 7-12, March 1960.
- [6] W. Sandrin *et al.*, "Aeronautical Satellite Data Link Study," *COMSAT Technical Review*, Vol. 15, No. 1, pp. 1-38, Spring 1985.
- [7] Y. Yasuda, K. Kashiki, and Y. Hirata, "High-Rate Punctured Convolutional Codes for Soft Decision Viterbi Decoding," *IEEE Transactions on Communications*, Vol. COM-32, No. 3, pp. 315-319, March 1984.
- [8] G. Clark, Jr., and J. Cain, *Error-Correction Coding for Digital Communications*, New York: Plenum Press, 1981.
- [9] Inmarsat, "Aeronautical System Definition Manual," 1992.
- [10] Y. Yasuda *et al.*, "Development of a Variable-Rate Viterbi Decoder and Its Performance Characteristics," 6th International Conference on Digital Satellite Communications, Phoenix, AZ, *Proc.*, pp. XII.24-XII.31, September 1983.
- [11] T. Mizuike and Y. Ito, "Optimization of Frequency Assignment," *IEEE Transactions on Communications*, Vol. 37, No. 10, pp. 1031-1041, October 1989.
- [12] H. Okinaka, Y. Yasuda, and Y. Hirata, "Intermodulation Interference-Minimum Frequency Assignment for Satellite SCPC Systems," *IEEE Transactions on Communications*, Vol. COM-32, No. 4, pp. 462-468, April 1984.

---

**Session 2**  
**Spacecraft Technology**

---

Session Chair—*Shuichi Samejima*, Nippon Telephone and Telegraph, Japan  
Session Organizer—*Alan Maclatchy*, Communications Research Centre, Canada

---

<b>The MSAT Spacecraft of Telesat Mobile Inc.</b> <i>E. Bertenyi</i> , Telesat Canada, Canada.....	41
<b>Adaptive Digital Beamforming for a CDMA Mobile Communications Payload</b> <i>Samuel G. Muñoz-García and Javier Benedicto Ruiz</i> , European Space Agency/ESTEC, The Netherlands .....	43
<b>Electrical Performance of Wire Mesh for Spacecraft Deployable Reflector Antennas</b> <i>Greg Turner</i> , Harris Corp., U.S.A. ....	45
<b>Adaptive Array Antenna for Satellite Cellular and Direct Broadcast Communications</b> <i>Charles R. Horton and Kenneth Abend</i> , GORCA Systems Inc., U.S.A. ....	47
<b>SAW Based Systems for Mobile Communications Satellites</b> <i>R.C. Peach, N. Miller and M. Lee</i> , COM DEV Ltd., Canada .....	53
<b>Broadband Linearisation of High-Efficiency Power Amplifiers</b> <i>Peter B. Kenington, Kieran J. Parsons and David W. Bennett</i> , Centre for Communications Research, England .....	59

